Instability of local supersonic regions on an airfoil with a spoiler

© A.G. Kuzmin

St. Petersburg State University,
198504 St. Petersburg, Russia
e-mail: a.kuzmin@spbu.ru

Received April 17, 2025
Revised July 15, 2025
Accepted July 25, 2025

The turbulent transonic airflow over NASA SC(2)-0710 airfoil with a spoiler is studied numerically. Solutions of the Reynolds-averaged Navier–Stokes equations are obtained with a finite-volume solver. The solutions reveal a high sensitivity of flow pattern to values of the spoiler deflection angle, as well as to changes in the freestream Mach number M_∞ and angle of attack α. The existence of lift coefficient hysteresis in narrow bands of M_∞ and α is shown.

Keywords: airfoil, transonic flow, shock waves, instability.

DOI: 10.61011/TP.2025.12.62492.216-25

Introduction

In previous years, numerical simulation of the flow over flaps and spoilers at fixed angles of deployment was performed in a number of studies [1]. In addition, the dynamics of the aerodynamic forces arising due to the unsteady behavior of the control surfaces was studied [2]. However, the structure of the flow in transonic conditions and its sensitivity to small disturbances have not been fully investigated.

The deployment of the spoiler causes a change in the profile of the wing, as a result of which the curvature of its upper side decreases or changes its sign, forming a concavity near the beginning of the spoiler. The transonic flow around profiles comprising parts of small curvature was studied in Ref. [3,4], where instability was shown to occur due to the fusion/splitting of emerging local supersonic zones. The transonic flow around the NASA SC(2)-0710 profile with a spoiler was numerically studied in Ref. [5] at its deflection from the neutral position by angles up to 6° and the Reynolds number $\mathrm{Re} = 1.5 \cdot 10^7$. The existence of a hysteresis of the lift force in certain intervals of variation of the free-stream Mach number M_∞ and the angle of attack α has been established.

In the present paper, similar issues are studied at a smaller Reynolds number $\mathrm{Re} = 9 \cdot 10^6$. The dependence of the lift coefficient C_L on M_∞ and α in the ranges $0.820 \le M_\infty \le 0.865$, $-0.55^\circ \le \alpha \le -0.25^\circ$ at the spoiler deflection angle $\theta = 3^\circ$ is analyzed.

1. Numerical method

The NASA SC(2)-0710 airfoil of thickness 10 % is defined by the table of dimensionless Cartesian coordinates $y_{\pm 0710}(x)$, $0 \le x \le 1$ [6], where „+“ and „–“ correspond to the upper and lower sides of the profile, respectively. Let's choose the chord length equal to $l_x = 2.5$ m and assume that the non-dimensionalization is performed by l_x. The model of the spoiler installed on the upper side of the profile in the range $0.55 \le x \le 0.77$ is described by the expressions [5]:

$$y_{+0710}(x) + (x - 0.55)\tan\theta$$

— for the outer side of the spoiler,

$$y_{+0710}(x) + (x - 0.55)\tan\theta - 0.0012$$

— for its inner side,
where θ is the angle of deflection from the neutral position (Fig. 1). The outer boundaries of the computational domain are the arcs of circles

$$\Gamma_1 : \; x(y) = 105 - (145^2 - y^2)^{1/2}$$

and

$$\Gamma_2 : \; x(y) = -105 + (145^2 - y^2)^{1/2},$$
$$-100 \le y \le 100, \quad -40 \le x \le 40,$$

located at a sufficiently large distance from the profile. At the inflow boundary Γ_1, the static temperature of the incoming air flow is set $T_\infty = 223.15$ K, turbulence level 1 %, Mach number $M_\infty < 1$ and angle of attack α, which determine the velocity components $U_\infty = M_\infty a_\infty \cos\alpha$, $V_\infty = M_\infty a_\infty \sin\alpha$, where a_∞ is the speed of sound. To study the effect of the Reynolds number (Re), a lower than in Ref. [5] pressure of $p_\infty = 13217$ Pa is set at the outflow boundary Γ_2; $\mathrm{Re} = \rho_\infty M_\infty a_\infty l_x/\mu \approx 9 \cdot 10^6$, where $\rho_\infty = 0.2060$ kg/m^3 is the air density and $\mu = 1.5 \cdot 10^{-5}$ kg/(m·s) is the dynamic viscosity. Conditions of no-slip and absence of heat flux are placed on the solid walls of the channel. Air is considered as a perfect gas with adiabatic constant of 1.4 and a specific heat capacity at constant pressure of 1004.4 J/(kg·K). The Sutherland formula is used to calculate the dynamic viscosity. The initial conditions are the parameters of the incoming flow or the flow field obtained with other values M_∞ and α.

Numerical simulation of two-dimensional turbulent flow was carried out on the basis of a system of unsteady-Reynolds-averaged Navier–Stokes equations. The turbulence model $k-\omega$ SST [7] was used. The sought-after parameters were the time-averaged values of static pressure $p(x, y, t)$, temperature $T(x, y, t)$, and the flow velocity components $U(x, y, t)$, $V(x, y, t)$. The solutions were obtained using the ANSYS-19.1 CFX software package based on the finite volume method [8]. A high-resolution [9] scheme was used to discretize convective terms, and time discretization was carried out using an Euler's implicit upwind scheme.

The calculations were performed using 3*D*-grid of 586,240 cells and consisting of 40 layers of parallelepipeds on the channel walls and prisms with triangular bases in the rest of the area. A single $l_z = 0.01$ m long cell was used over the computational domain in the direction of the axis z. The grid nodes condensed near the shock waves, in the boundary layer, and in the near wake. The dimensionless thickness $y+$ of the first grid layer on the profile was less than one. Test calculations on different grids have shown that the above grid provides a fairly good accuracy of numerical solutions [5, Fig. 3].

2. Results

The obtained solutions to the initial boundary value problem under stationary boundary conditions converged in time to the stationary distributions of the parameters $p(x, y)$, $T(x, y)$, $U(x, y)$, $V(x, y)$. In the case of $M_\infty = 0.81$, $\alpha = 0°$ and the neutral position of the spoiler $\theta = 0°$, the formation of a local supersonic zone Z_{upper} of significant size on the upper side of the profile was documented. Integrating the pressure $p(x, y)$ over the profile allows one to find the lift force $L = 137.2$ N, as well as the lift force coefficient $C_L = 0.594$, according to the formula $C_L = 2L/[\rho_\infty (U^2)_\infty S]$, where $S = l_x \times l_z = 2.5 \times 0.01\,\text{m} = 0.025\,\text{m}^2$ is the projection area of the l_z thick profile onto the plane (x, z).

The deflection of the spoiler from the neutral position by an angle $\theta = 3°$ causes a deceleration of the flow along the upper side of the profile, a decrease in the size of the local supersonic zone Z_{upper} and its splitting into two parts (Fig. 1), where SW means a shock wave. In this case, the lift force coefficient is equal to 0.417.

A further increase in the angle of rotation of the spoiler θ from 3 to 6° at $M_\infty = 0.81$, $\alpha = 0°$ leads to a decrease in the value of C_L from 0.417 to 0.124. Pulse angle switching θ in time from 0 to 3° and back with a period of 0.5 s causes fluctuations in the lift coefficient within $0.37 \le C_L \le 0.65$; when switching θ the flow field obtained over the time of 0.5 s for the previous value of θ was used as the initial condition.

An increase in M_∞ and/or a decrease in the angle of attack is accompanied by the formation of a local supersonic zone Z_{lower} on the lower side of the profile.

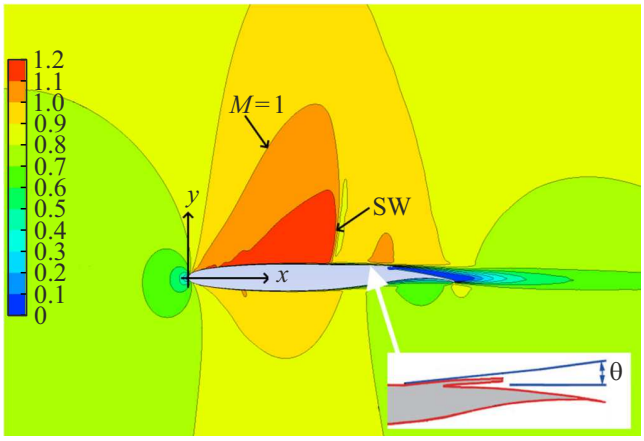

Figure 1. Contours of the Mach number $M(x, y) = \text{const}$ for $M_\infty = 0.81$, $\alpha = 0°$ and the deflection of the spoiler by an angle $\theta = 3°$.

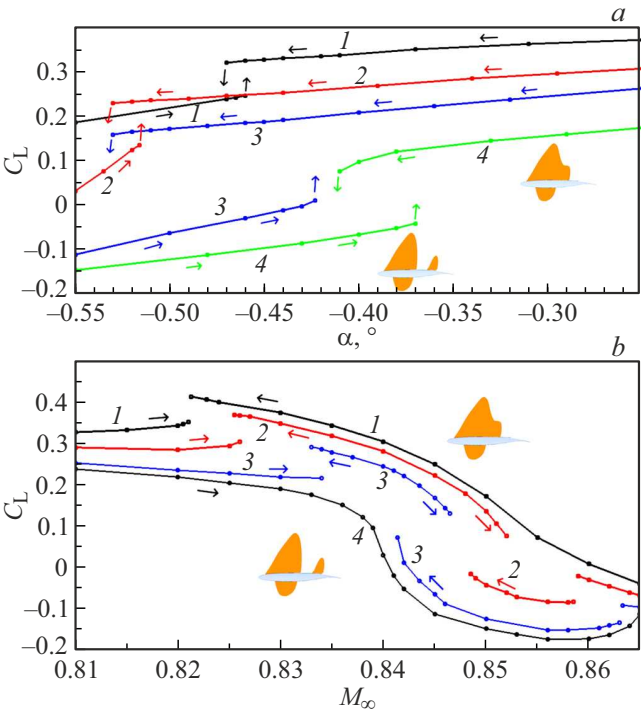

Figure 2. Lift coefficient C_L at the angle of deflection of the spoiler $\theta = 3°$: *a* — dependence of C_L on the angle of attack α, the curves *1–4* correspond to $M_\infty = 0.830$, 0.840, 0.845, 0.850; *b* — dependence of C_L on the Mach number M_∞, curves *1–4* correspond to the angles $\alpha = -0.25°$, $-0.37°$, $-0.50°$, $-0.55°$.

The interaction of the zones Z_{upper} and Z_{lower} leads to a very complex behavior of C_L at changes in the parameters of the incoming flow in the ranges $-0.55° \le \alpha \le -0.25°$, $0.852 \le M_\infty \le 0.864$. Fig. 2, *a* shows the obtained dependences of the lift coefficient C_L on the angle of attack α at $\theta = 3°$ and different values of M_∞. The arrows near the curves indicate the directions of step-by-step change in α. The flow field obtained in the previous step was used as

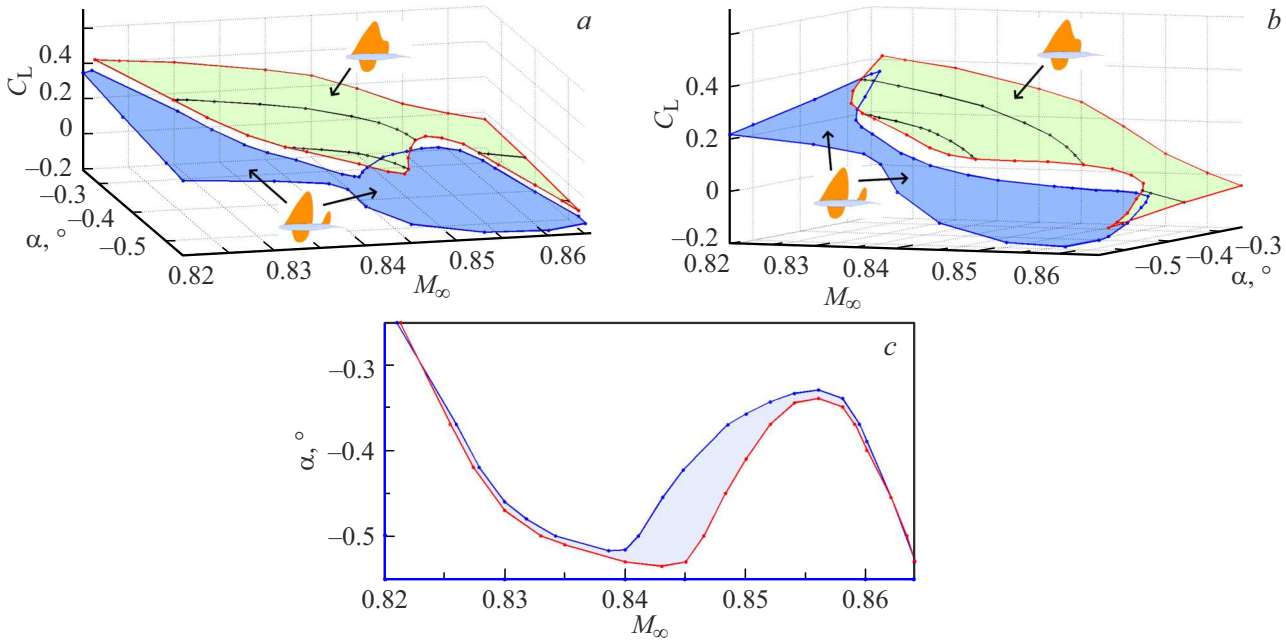

Figure 3. *a, b* — surfaces illustrating the dependence of the lift coefficient C_L on the Mach number M_∞ and the angle of attack α at $\theta = 3°$; *c* — bifurcation curves on a plane (α, M_∞).

the initial condition at each step. The upper branches of the curves correspond to flow patterns with one supersonic zone on the profile, and the lower branches with two supersonic zones, which is illustrated by sketches located near the curve *4*. The transitions between the branches are accompanied by jumps C_L caused by the instability of the coalescence/splitting process of supersonic zones and a sharp change in the position of the SW shown in Fig. 1. As seen there is hysteresis during the transition from the lower branches to the upper branches and vice versa. The largest hysteresis width is observed at $M_\infty = 0.845$.

Fig. 2, *b* shows the dependences of C_L on the Mach number M_∞ at different values of the angle of attack. The transitions from the lower branches of the curves *1–3* to the upper ones with an increase in M_∞ from 0.82 to 0.84 are explained by the merger of two local supersonic zones on the upper side of the profile and the formation of a large supersonic zone Z_{upper} with a reduced static pressure. With a further increase in M_∞ , an abrupt drop of C_L is realized in the range $0.845 < M_\infty < 0.853$, caused by splitting the zone Z_{upper} into two parts. Splitting occurs due to the deceleration of the flow at the trailing edge of the profile due to the displacement of the streamlines in the near wake „up“ similar to the rotation of the flap counterclockwise [5]. The displacement of the streamlines, in turn, is caused by a sharp expansion of the supersonic zone Z_{lower} on the lower side of the profile and a shift in the separation point of the boundary layer to the trailing edge.

Fig. 3, *a* and *b* show a surface illustrating the dependence of the lift coefficient C_L on two parameters — α and M_∞ — for $\theta = 3°$. The surface consists of lower and upper parts, the projections of which on the plane (α, M_∞) overlap due to hysteresis. The upper part of the surface corresponds to flow patterns with one supersonic region on the upper side of the profile, and the lower — flow patterns with two supersonic regions on the upper side.

Fig. 3, *c* shows bifurcation curves obtained by projecting the edges of the surface $C_L(\alpha, M_\infty)$ onto the plane (α, M_∞). In the shaded area, the projections of the upper and lower parts of the surface $C_L(\alpha, M_\infty)$ overlap, so there are two flow modes for the values α and M_∞ from this area. A comparison with the results obtained in Ref. [5], shows that the hysteresis width increases significantly with a decrease in pressure p_∞ and a decrease in the Reynolds number; in particular, at $M_\infty = 0.845$, the hysteresis width with respect to the angle of attack is 0.1°.

Acknowledgments

The study was performed using the resources of the computing center of St. Petersburg State University (http://cc.spbu.ru).

Conflict of interest

The author declares that he has no conflict of interest.

References

[1] A. Petrocchi, G.N. Barakos. AIAA Paper, **2023**, 3527 (2023).
[2] S. Geisbauer. AIAA Paper, **2023**, 4316 (2023).
[3] A.M. Chuen, M. Hafez. Int. J. Aerodynamics, **7** (2), 127 (2021) (in Russian).
[4] A. Kuzmin. J. Phys. Conf. Ser., **1697**, ID 012207 (2020).

[5] A. Kuzmin. Int. J. Aeronautical Space Sci., **15** (3), 232 (2014).
[6] Ch.D. Harris. NASA Technical Paper, **2969**, Langley Research Center (1990).
[7] F.R. Menter. https://turbmodels.larc.nasa.gov/sst.html (accessed April 15, 2025)
[8] *ANSYS Fluids — Computational Fluid Dynamics*. https://cae-expert.ru/product/ansys-cfd (accessed April 15, 2025)
[9] T. Barth, D. Jespersen. AIAA Paper, **89**, 0366 (1989).

Translated by A.Akhtyamov